Paper No.
05562

CORROSION 2005

ANALYSIS OF A SEIZED CA6NM PLUG AND CAGE CONTROL VALVE IN HYDROPROCESSING SERVICE

D. W. Alley, S. A. Bradley and M. W. Mucek
UOP LLC.
25 E. Algonquin Rd.
Des Plaines IL 60017
e-mail: david.alley@uop.com

ABSTRACT

The results of an analysis of a CA6NM plug and cage control valve which seized in hydroprocessing service are presented. The valve was found to have seized due to the accumulation of corrosion deposits resulting from a relatively brief exposure to a high temperature hydrogen / hydrogen sulfide environment. Wear surfaces on the valve were nitrided to prevent galling. Nitrided surfaces were found to have a significantly lower corrosion resistance than predicted by the Couper-Gorman curves for 12 Cr stainless steels. This high corrosion rate is explained by depletion of chromium in solution due to the formation of chromium nitrides.

Keywords: CA6NM, hydroprocessing, nitriding, galling, hydrogen, hydrogen sulfide

INTRODUCTION

Following the commissioning of a new hydroprocessing unit at a Middle Eastern refinery in July 2001, seizures of control valves for the recycle gas heater were reported in January, April, and June of 2002. On stream time between the January, April, and June failures was about 60 days in each case. No abnormal operating conditions were reported during these periods. Figure 1 is a diagram showing the general arrangement of the unit and the location of the valve bank. The normal recycle gas stream is composed of 90% hydrogen, 3 – 4% hydrogen sulfide and 6 – 7% light hydrocarbon. The normal operating pressure and temperature of the recycle gas stream at the location of the valve bank were 17.25 MPa (2500 psi) and 400^{o} C (752^{o} F) respectively.

The valve bank, shown in Figure 2, consisted of ten - 10 cm (4 inch), balanced, plug and cage valves, mounted in parallel. The purpose of the valves was to ensure uniform flow distribution to the ten heater passes. Seizure of the valves resulted in the inability of the refinery to balance the flow between heater passes and created the potential for maldistribution of flow within the furnace. The refinery was, however, able to operate the unit for some time at full capacity following the seizures. The valves were

designed for automatic control but were often controlled manually. Figure 3 is a cross section of the valves showing the valve body, the trim (plug and cage) and the seat. The recycle stream enters the valve from the left, passes through the holes in the cage into the center of the cage and then exits the valve to the right. Throttling of the flow is accomplished through up and down movement of the plug which covers or exposes the holes. The plug has holes in its upper surface which allow gases to pass to and from a dead space under the valve bonnet. This ensures that pressures on both sides of the plug are equal and minimizes the forces required to move the plug.

The valve bodies were constructed from type 347 stainless steel (UNS S34700). The seat and the stem were constructed from type 316 stainless steel (UNS S31600). Portions of the seat which were directly exposed to the process gases were weld overlayed with UNS R30006 (cobalt based hardfacing alloy) to provide wear resistance. The valve trim (plug and cage) were cast martensitic stainless steel, CA6NM (UNS J91540)(12% Cr, 4% Ni). Sliding surfaces of the plug and cage were nitrided to provide resistance to galling. The trim material and nitriding process were selected by one or more of the involved parties based on the inclusion of this material and treatment in NACE Standard MR0175-98[1] (paragraph 3.7.2.1 and 7.2). (NACE Standard MR0175 has been superseded by NACE Standards MR0175/ISO15156 for oilfield applications and MR0103-2003 for refinery applications).

The seizing problem was resolved by changing the type of valve (balanced plug and cage to unbalanced plug) and trim material (nitrided CA6NM to type 347 stainless steel). No related failures have been reported elsewhere in this unit or in this location since the valves were replaced.

EXPERIMENTAL DETAILS

A variety of experimental techniques were employed in this investigation. Primary techniques included visual observations, light microscopy, electron microscopy, energy dispersive spectroscopy (EDS), wavelength dispersive spectroscopy (WDS), microhardness testing (Vikers, 500g load), inductively coupled plasma spectroscopy (ICP) and X ray diffraction. Standard techniques and instrument settings were used in all instances.

RESULTS

Visual Observations

Figure 4 shows a typical valve trim as received. There was some variation in the hole pattern and construction of the trims examined; however, these differences were not significant to the seizure of the valves or the resolution of this problem. The valve seat may be seen at the bottom of the trim, and the bottom of the plug may be seen through the holes in the cage. Significant amounts of gray scale are present on most surfaces of the plug and cage. Some of the scale had a, faceted, crystalline appearance.

The process of disassembling the valve trims required the use of a great deal of force. Upon disassembly significant quantities of gray scale fell from the gap between the cage and the plug. This scale was similar in appearance to that observed on the outside of the cage. Figure 5 shows a typical trim following disassembly. Figure 6 shows a close up view of the plug. Scale thicknesses varied with location due to clearances within the valve but are 2 – 3 mm thick at the location shown by the arrow.

Metallography

Figure 7 is a micrograph showing the typical structure of the base metal of the plug and cage. The structure is martensitic as is expected for CA6NM material.

Figure 8 is a micrograph of a typical surface region of the trim. Base metal, as shown in Figure 7, is designated "A" in this figure. "B" is a dark band which was originally believed to be the nitrided layer, but as will be shown in the chemistry section below, proved to be a carburized layer. Again, as will be shown in the chemistry section below, layers D and E are chromium rich and iron rich sulfides respectively. Mounting media is visible in the upper left corner of the micrograph.

Figure 9 shows the corner of the cage where it meets the seat. The vertical portion of the cage at the right of the micrograph is exposed to the process environment. The horizontal portion of the cage at the bottom of the micrograph mates with the seat and is protected from the process environment. The microstructure of the base metal, labeled "A" in this Figure is different from that shown in Figure 7. The microstructure in this Figure is dendritic while that in Figure 7 is martensitic. Whether the final CA6NM casting appears martensitic or dendritic depends on a number of factors such as chemistry, cooling rate, and post casting heat treatments. It is not clear why the structure is different in two otherwise similar castings, however, the state of the base metal, martensitic or dendritic, did not contribute to the seizure of the valves. The inner and outer (chromium and iron rich) sulfide layers, labeled "D" and "E", are visible in areas where the cage was exposed to the process environment (right side of micrograph) and absent where the cage was protected from the environment. The dark, carburized layer in this figure ("B") is uniform in thickness regardless of the presence or absence of sulfide scales and is of similar thickness to the typical dark layer shown in Figure 8. An additional layer "F", which is not present in Figure 8, is visible in this micrograph in locations protected from the process environment. As will be shown in Figure 10, hardness tests, and the chemical analyses section below, this is the nitrided layer.

Microhardness Testing

Figure 10 is a micrograph showing the results of microhardness testing (Vickers 500 g load). As in previous micrographs, "A" represents base metal (dendritic in this case); "B" represents the carburized layer; "F" represents the nitrided layer; and "D" represents the chromium rich sulfide layer. Hardness values for the various layers may be found in Table 1. All hardness values were within the expected ranges.

Chemical Analyses

Table 2 contains the chemical analyses of the plug and cage base metal as determined by inductively coupled plasma spectroscopy (ICP) and the ASTM requirements for CA6NM material. The chemical analyses of the plug and cage were consistent with the chemistry requirements for CA6NM material.

Figure 11 shows the variation in chemical composition of nickel, chromium, iron and sulfur for the scale and near surface based metal at a location where the nitrided layer was not present. This figure indicates that the outer layer "E" is an iron rich metal sulfide and that the inner layer of scale "D" is a chromium rich metal sulfide. This scale configuration (composition and layer structure) is typical of sulfide scales formed at high temperature hydrogen sulfide environments.

Figure 12 shows the variation in carbon and nitrogen through the nitrided layer ("F"). This Figure shows that the region of increased nitrogen is very well defined and is in the location indicated by Figure 8. It also shows that there is some increase in carbon associated with the nitrided layer but that the carbon concentration is not solely related to the nitride layer, i.e., the variability in carbon concentration is much less distinct than the variation in nitrogen concentration.

DISCUSSION

As stated in the introduction, the purpose of the valves was to control the flow of recycle gas to ensure uniform flow to the 10 heater passes. The valves were designed to accomplish this task through the vertical motion of the plug within the cage. This motion either covered or uncovered holes in the cage and thereby regulated flow. The design of the valve required relatively tight tolerances and frequent motion between the cage and the plug. The seizure of the valves is attributed to higher than expected corrosion rates and the resultant accumulation of corrosion products between the cage and plug. A corrosion mechanism which accounts for the greater than predicted rates of corrosion is proposed below.

The basis used for the selection of nitrided CA6NM valve trim for this service is not clear. There is some evidence that the material and surface treatment were selected based on their inclusion in MR0175-98 despite the fact that MR0175-98 is applicable only to sulfide stress cracking (not corrosion) in aqueous environments (paragraphs 1.1 – 1.3).[1] If predicted corrosion rates formed the basis for selection, it is probable that the Couper-Gorman curves[2] (Figure 13) for the corrosion of 12% chromium steels in H_2/H_2S service were used. These curves predict a corrosion rate of 0.3 mm/yr (11 mpy) for this service (3 – 4% H_2S at 400^{o}C [752^{o}F]).

Given that the seizure appeared to be due to the excessive accumulation of corrosion products, the determination of the actual corrosion rates for the parts was considered relevant. Two approaches were available. One approach relied on the uniformity of the carburized layer while the other is based on the thickness of the dense inner scale ("D").

Analytical results indicate that the dark layer ("B") shown in Figure 9 is a carburized layer. Given that the operating temperature of the valves is too low to cause significant carburization, this layer must have formed in association with nitriding process. (It is unlikely that the carburized layer is an intentional result of the nitriding process as most nitriding processes such as ion nitriding and ammonia gas nitriding do not involve carbon. Carbon contamination on the surface of the part could account for the carburized layer.) As such, the thickness of this layer is expected to be equal at all locations on the part. Careful examination of Figure 9 indicates that, following exposure, the thickness of the carburized layer remains uniform irrespective of the presence or absence of the nitrided layer ("F") or sulfide scales ("D" and "E"). The presence of the nitrided layer over the carburized layer at some locations indicates that the carburized layer has not been corroded in these locations. The uniformity of the thickness of the carburized layer between locations where the nitrided layer is present and absent indicates that the carburized layer has not been corroded even in areas where the nitrided layer is absent. From this it may be inferred that the thickness of material corroded in areas from which the nitrided layer is absent is exactly equal to the thickness of the nitrided layer. The thickness of the nitrided layer was specified to be 0.15 mm. The corrosion rate resulting from the loss of 0.15 mm in two months of service is 0.9 mm/yr (35 mpy).

Calculation of the corrosion rate based on scale thickness involves determining the amount of material which is required to corrode to produce the observed scale. The typical thickness of the inner

scale ("D") was approximately 0.4 mm. Based on the molar volumes iron (7.1 cm^3/mole) and FeS (20.6 cm^3/mole for a scale which is 90% dense), approximately 0.14 mm of iron is required to corrode to produce the observed scale. The corrosion rate calculated in this manner is 0.84 mm/yr.

The close agreement between the corrosion rate calculated from the loss of the nitrided layer (0.9 mm/yr [35 mpy]) and that calculated from scale thickness (0.84 mpy [33 mpy]) and the large difference between these values and the corrosion rate predicted by the Couper-Gorman curves (0.3 mm/yr [11 mpy]) makes it highly unlikely that observed difference in the values is due to statistical or measurement uncertainty. A difference in the corrosion of CA6NM, as predicted by the Couper-Gorman curves and nitrided CA6NM, as measured in this study, must be determined.

The purpose of nitriding is to form a hard surface. This is accomplished by a chemical reaction between chromium and nitrogen to form chromium nitrides. This reaction result in a reduction of chromium in solution. The corrosion resistance of stainless steels to high temperature environments is determined by the concentration of chromium in solution rather than the total chromium present in the alloy. This is precisely the same mechanism responsible for intergranular corrosion following sensitization, however, sensitization is limited to grain boundaries while nitriding reduces the levels of chromium in solution, and thereby corrosion resistance, throughout the grain. Given that the nitriding process has significantly reduced the concentration of chromium in solution in the nitrided layer, it would be more appropriate to estimate the corrosion rate for this layer using the Couper-Gorman curves appropriate to the chromium remaining in solution. Use of the 12 Cr curve remains appropriate for the remainder of the bulk material. The 0 – 5 Cr Couper-Gorman curve is Figure 14. Using this Figure, a corrosion rate of approximately 1 mm/yr (40 mpy) is predicted for the operating conditions in question. This predicted corrosion rate is only slightly higher than that observed in this investigation which indicates that the nitriding process reduced the chromium in solution in the nitrided layer from approximately 13% to near 5%. This reduction in chromium in solution increased the corrosion rate for the nitrided layer from 0.3 mm/yr (11 mpy) to 0.9 mm/yr (35 mpy). There is no evidence from this investigation that there was any increase in the corrosion rate of the non-nitrided CA6NM or that the Couper-Gorman curves do not accurately predict the corrosion rate of non-nitrided CA6NM. Furthermore, this study indicates that the Couper-Gorman curves accurately reflect the corrosion rates of steels based on the level of chromium in solution.

CONCLUSIONS

1. The seizure of the control valves was caused by the accumulation of corrosion deposits.

2. The corrosion rate experienced by the nitrided layer was in line with that which would be predicted by the Couper-Gorman curve for 0 – 5 Cr steel and much higher than would be predicted for 12 Cr steel.

3. The discrepancy in the corrosion rates is due to the nitriding process in which chromium nitrides are formed. The formation of chromium nitrides depletes the chromium in solution in much the same manner as the process of sensitization in stainless steels. The reduction of chromium in solution is responsible for the accelerated corrosion.

4. Materials for this environment were specified through the application of MR0175 to environments beyond its scope.

5. There is nothing in this investigation which would indicate that the misuse of MR0175 was unique to this case. This indicates the potential presence of a communication gap between the document and its

users. Whether this gap is attributable to the document or to its users and whether a potential communication gap continues to exist between replacement documents and their users was not considered in this investigation.

REFERENCES

1. NACE Standard MR0175-98, Standard Material Requirements, Sulfide Stress Cracking Resistant Metallic Materials for Oilfield Equipment (NACE International, Houston TX, 1998)

2. A. S. Couper and J. W. Gorman, Computer Correlations to Estimate High Temperature H_2S Corrosion in Refinery Streams, Materials Protection and Performance, January 1971

Table 1 Vickers microhardness values (500g load).
Letter designations refer to Figure 10

Letter Designation	Layer Composition	Hardness (HV)
A	CA6NM Base Metal	353 - 380
B	Carburized Layer	380 - 419
F	Nitrided Layer	1080

Table 2 Chemical analyses (ICP) of plug and cage and ASTM standard for CA6NM (heat analysis requirement)

Element	Cage	Plug	ASTM A487-CA6NM
Carbon	0.04	0.04	0.06 max.
Manganese	0.81	0.82	1.00 max.
Phosphorous	0.027	0.026	0.04 max.
Silicon	0.23	0.21	1.00 max.
Nickel	3.6	3.4	3.5-4.5
Chromium	11.8	12.0	11.5-14.0
Molybdenum	0.51	0.50	0.4-1.00
Vanadium	0.04	0.04	0.05 max.

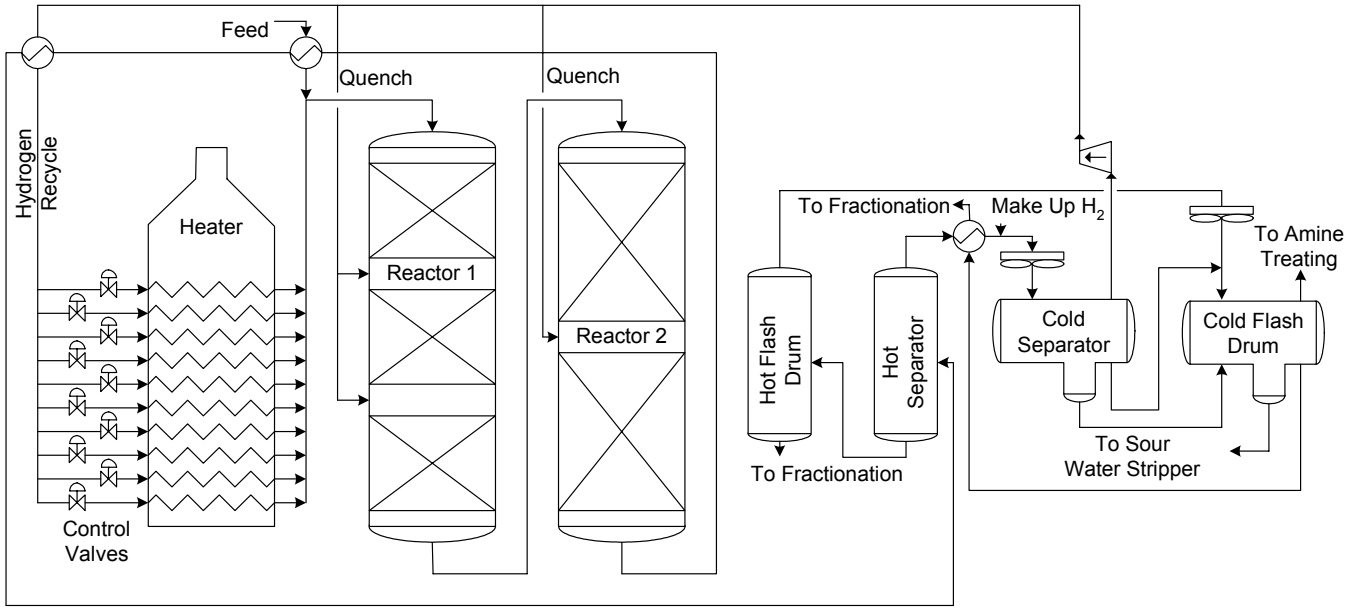

Figure 1 Diagram showing flow scheme for hydroprocessing unit and location of recycle gas heater control valves.

Figure 2 Photo of valves.

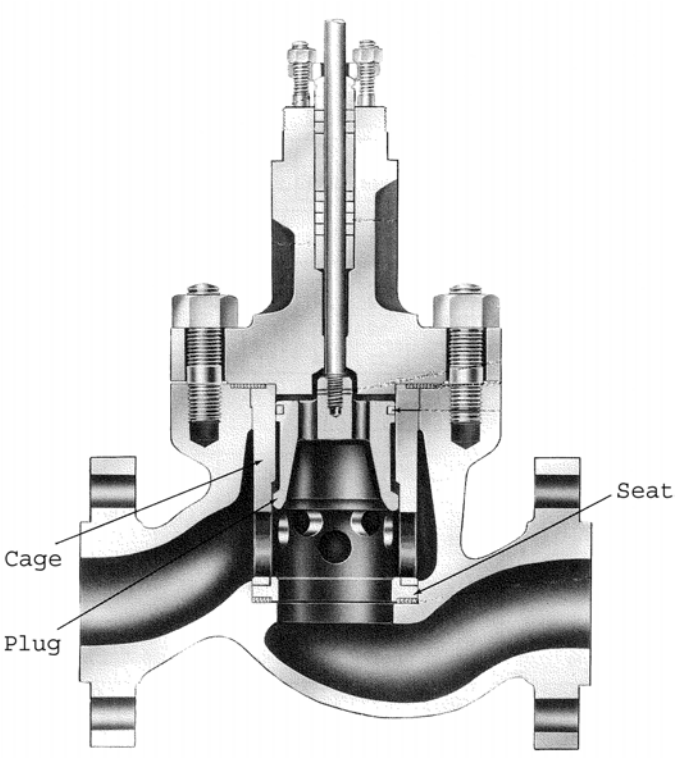

Figure 3 Control valve cross section.

Figure 4 Typical valve trim. Seat is visible at the bottom of the trim. Plug is visible through holes in cage.

Figure 5 Typical valve trim following disassembly. Pressure equalization holes are visible in the top of the plug.

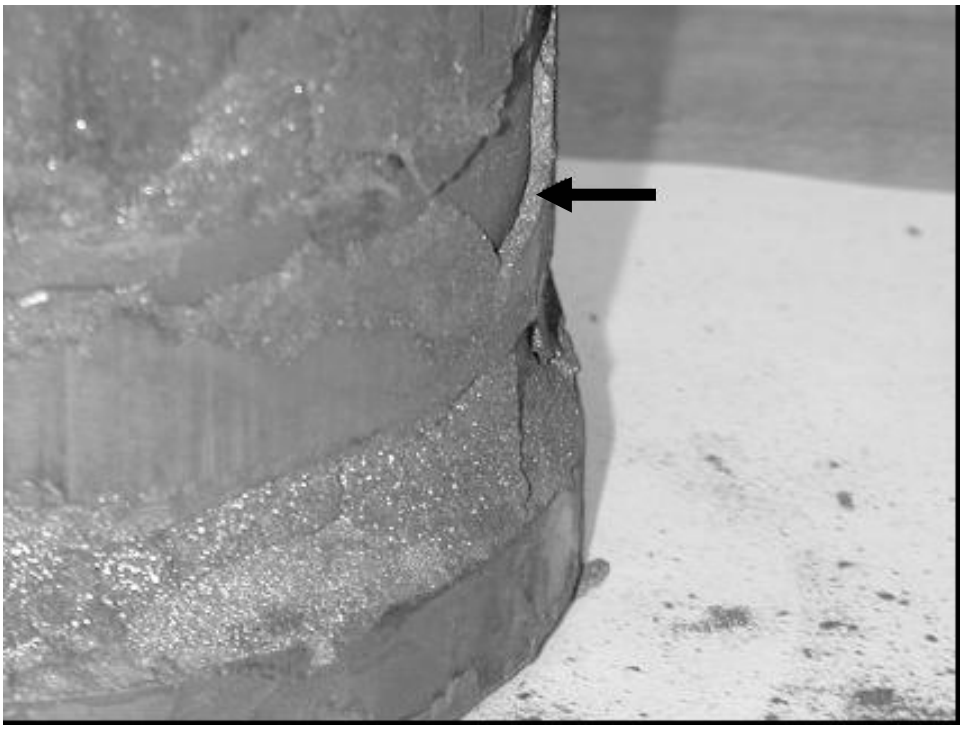

Figure 6 Close-up view of plug. Scale spalled in several locations. Scale thickness at arrow is 2 – 3 mm.

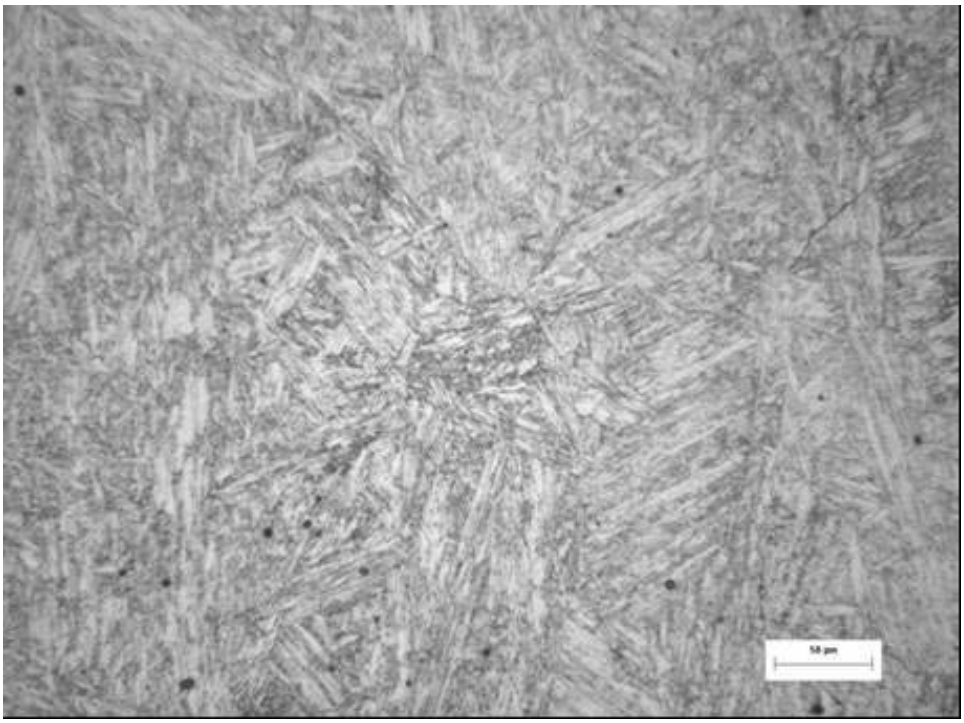

Figure 7 Micrograph of cage base metal showing martensitic structure.

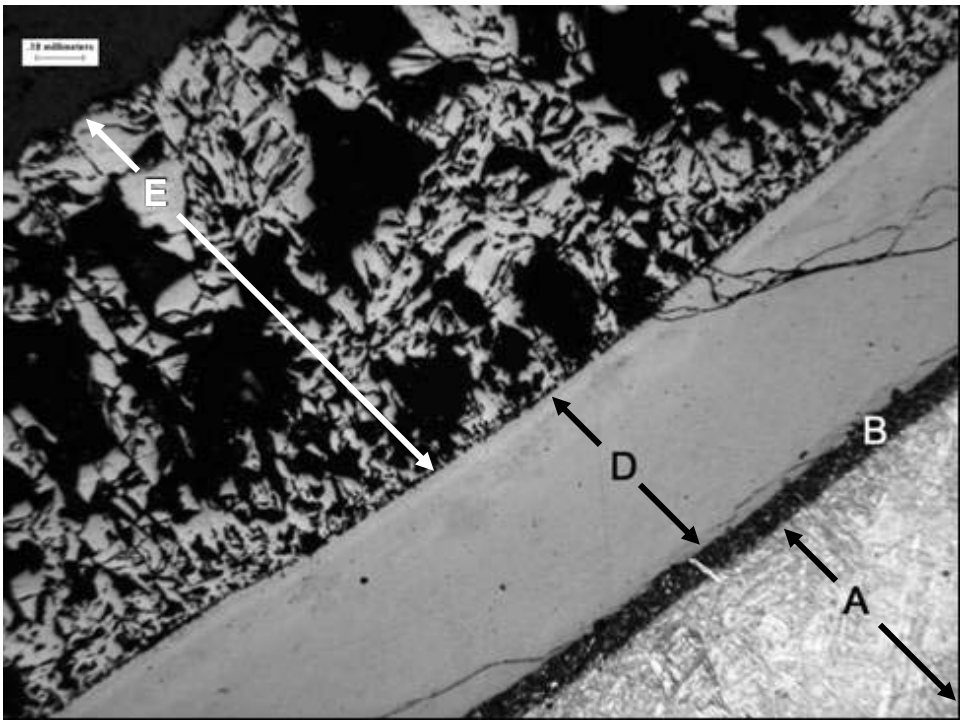

Figure 8 Micrograph of a typical surface region of the trim. "A" is martensitic base metal, "B" is the carburized layer, "D" is a Cr rich sulfide, "E" is an iron rich sulfide.

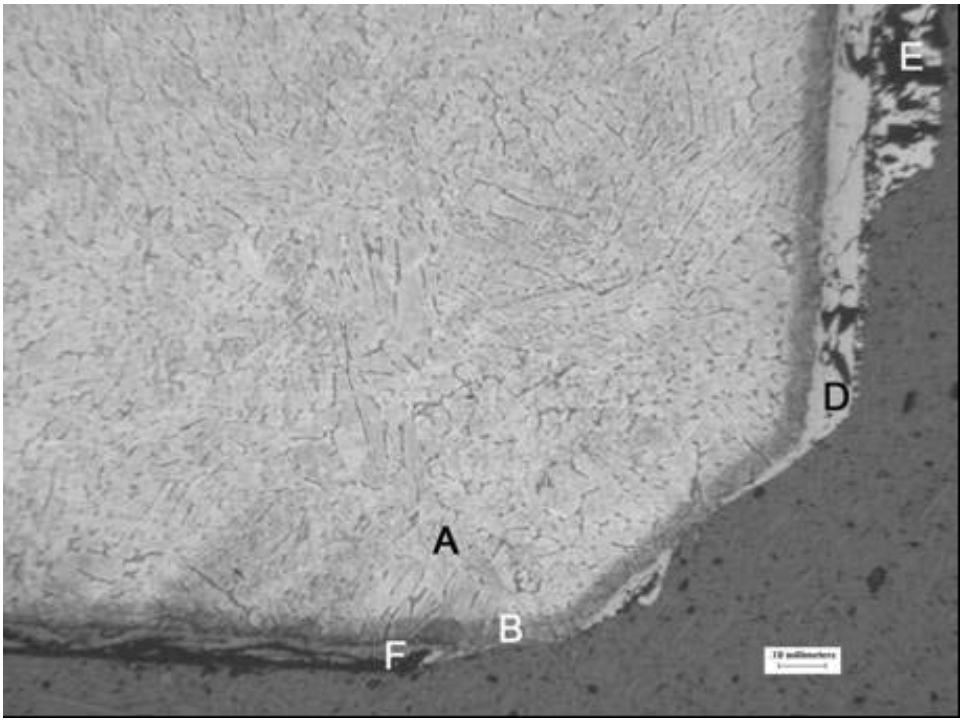

Figure 9 Micrograph of corner of cage. Right edge exposed to process. Bottom edge protected by seat. Symbols as identified in Figure 8. "F" is the nitride layer.

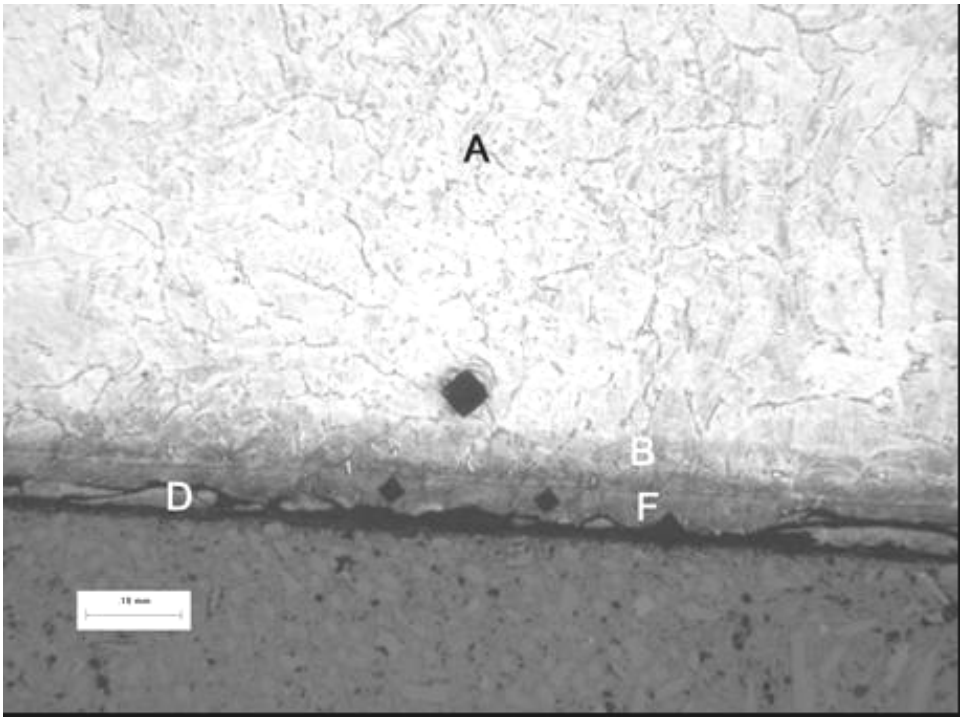

Figure 10 Vickers microhardness indents showing the variation in hardness between the base metal "A" and the nitrided layer "F".

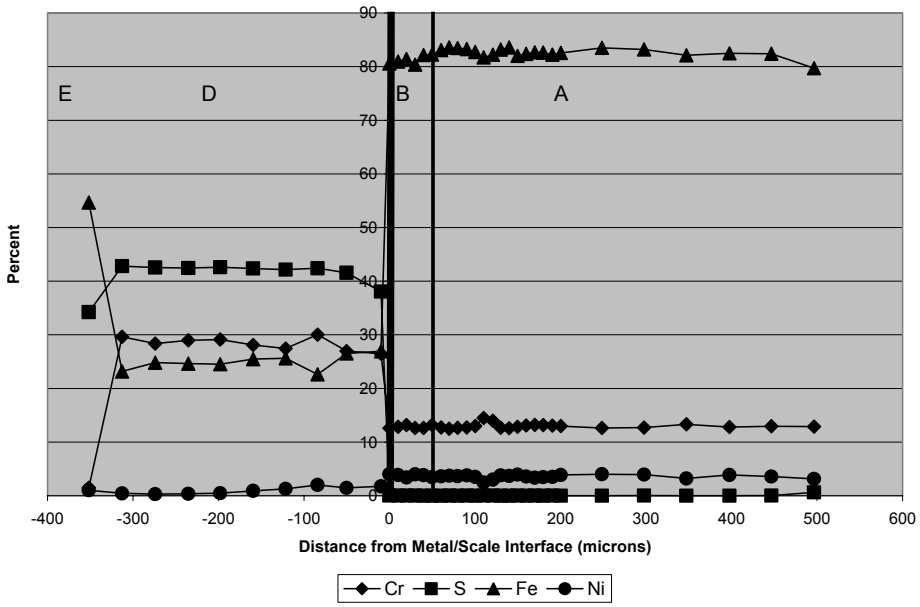

Figure 11 Variation in chemical composition with distance. Letters refer to bands as in previous Figures.

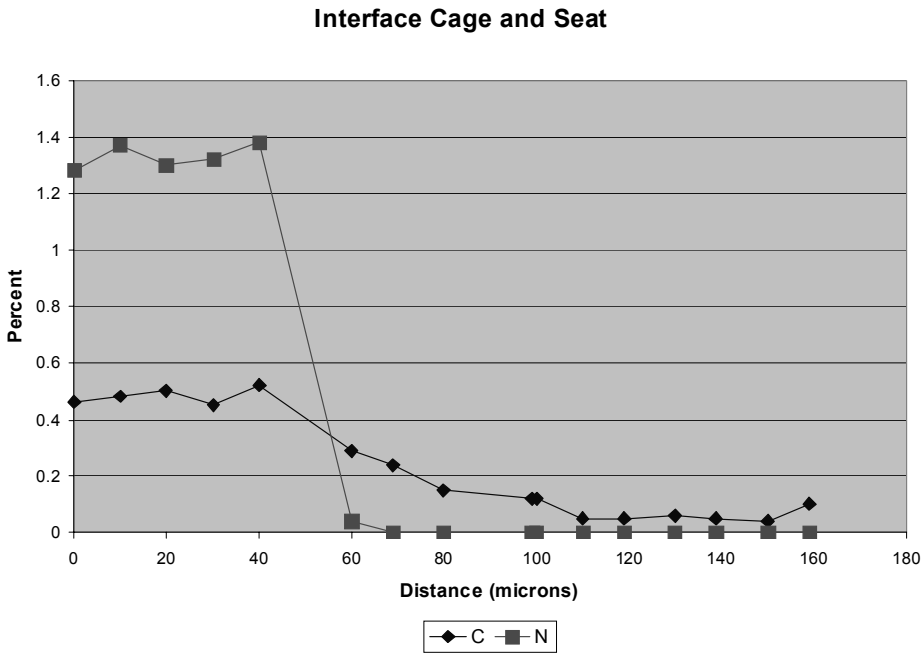

Figure 12 Variation of carbon and nitrogen through the nitrided layer.

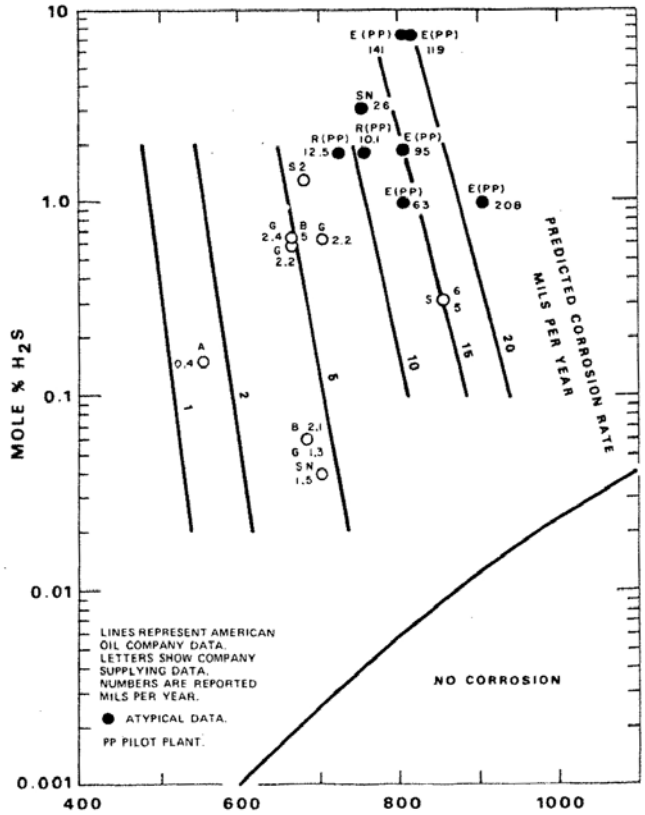

Figure 13 Couper-Gorman curve, 12 Cr stainless steel.[2]

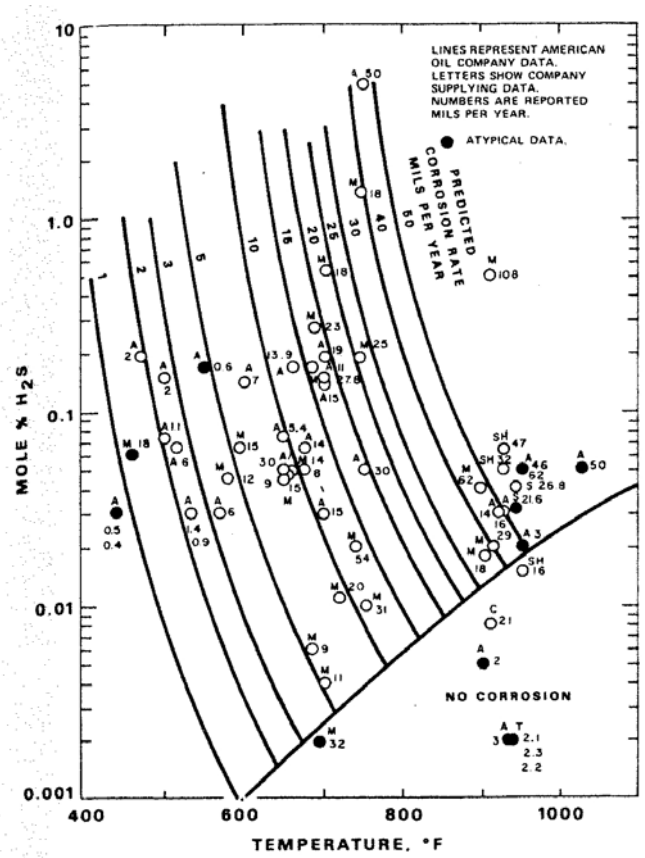

Figure 14 Couper-Gorman curve, 0 – 5 Cr steels.[2]